

Performance Analysis of TBR Tire Curing Process

D. B. Jani¹, S. B. Dikshit², N. J. Vadera³

Department of Mechanical Engineering (CAD\CAM)

Associate Professor, Department of Mechanical Engineering^{1,3}

P.G. Scholar, ME (CAD\CAM), Department of Mechanical Engineering²

Government Engineering College Dahod, Gujarat, India

dbjani@rediffmail.com and vaderanilesh97@gmail.com

Abstract: Numerical algorithms and computer programs have been developed to determine optimal cure steps in a tire curing process. A dynamic constrained optimization problem was formulated with the following ingredients: (1) an objective function that measures product quality in terms of final state of cure and temperature history at selected points in a tire; (2) constraints that consist of a process model and temperature limits imposed on cure media; (3) B-spline representation of a time-varying profile of cure media temperature. The optimization problem was solved using the complex algorithm along with a finite element model solver. Numerical simulations were carried out to demonstrate the procedure of determining optimal cure steps for a truck/bus radial tire. © 1999 John Wiley & Sons, Inc. *J Appl Polymer Sic* 74: 2063–2071, 1999.

Keywords: tire curing process; cure steps; state of cure; dynamic optimization; B- spine

I. INTRODUCTION

The curing process is the final step in tire manufacturing, whereby a green tire built from layers of rubber compounds is formed to the desired shape in a press. A schematic cross section of a dome-type cure press is shown in Figure 1. In the press, heat is transferred to the green tire from the mold and the bladder, which are kept at higher temperatures by circulated cure media like steam or hot water. The transferred heat provokes the curing reaction of the rubber compounds, thus converting the compounds to a strong, elastic material to meet tire performance needs.

The major operating variables of the curing process are the conditions of the supplied cure media, which are to be varied according to prescribed cure steps. It is desirable to adjust the temperature and Pressure of the cure media as a function of time so that the rubber compounds may attain specified levels of the state of cure (SOC). But in practice, the distributed nature of the heat transfer mechanism makes it difficult to have every compound reach the respective target level. Inside layers of a tire cannot be fully cured without causing the overcure of surface layers and the consequent reversion of vulcanized crosslink. Accordingly, there arises a need to make trade-offs between different parts of the tire with respect to the attainable SOC levels and other product quality measures, like temperature history during cure.

The conventional method to set up cure steps is to directly measure the temperature–time profiles using the thermocouples inserted into various parts of a green tire and then to convert the measured profiles to the SOC on the basis of some assumed cure kinetics.¹ This procedure has to be repeated several times with the cure steps altered each time until reasonable trade-offs are made. Thus, there has been a need to develop an alternative method that would replace the costly and time-consuming thermocouple experiments

The purpose of this study is to develop a numerical optimization procedure for determining optimal cure steps for product quality in a tire curing process. A dynamic optimization problem is formulated to optimize a measure of product quality in terms of the final state of cure and the temperature history at selected points in a tire. The optimization is carried out with the process model and the temperature limits of cure media as constraints. The time-varying profile of cure media temperature is discretized using B-spline. Then the optimization problem is solved using the complex algorithm along with a finite element model solver. Numerical simulations are presented to demonstrate the procedure of determining the optimal cure steps for a truck/bus radial (TBR) tire.

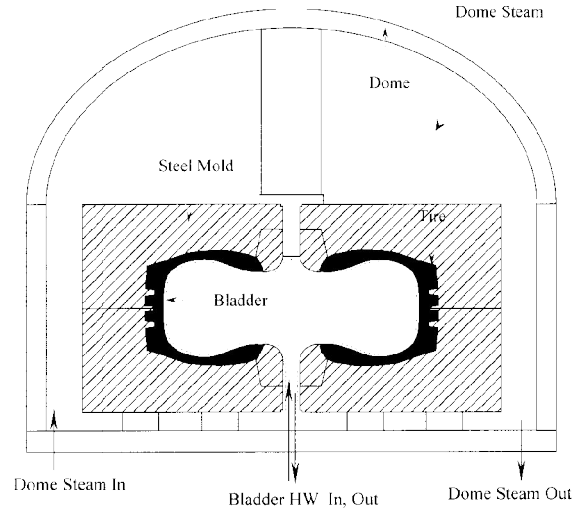


Figure 1 Schematic cross section of a dome-type cure press.

PROBLEM FORMULATION

Cure Optimization Problem

The state of cure represents the single most important measure of tire product quality as far as the curing process is concerned. The optimal product quality postulated in this study is to make the final states of cure of the selected rubber compounds approach their respective target values in a coordinated fashion. Another factor that affects the product quality is the temperature history experienced by heat-sensitive materials within tire during the cure: the temperature of composite layers should not exceed respective prescribed limits in order not to cause the deterioration of adhesion force. Now the problem of determining optimal cure steps for product quality in a curing process can be formulated as an optimization problem as follows:

$$\text{Minimize } J = J_x + rJ_t$$

$$= \frac{1}{n} \sum_{t=1}^n (x(t) - x^{set})^2 + \frac{r}{m} \sum_{j=1}^m \int_0^{t_j} [\max(T(t) - T_{set}^j, 0)]^2 dt \quad (1)$$

Subject to $f(x, T, T_m(t)) = 0$ for $0 \leq t \leq t_y$ (2)

$T_{m,l} \leq T_m(t) \leq T_{m,u}$ for $0 \leq t \leq t_h$ (3)

where J is the objective function, j is the measure of product quality in terms of SOC, J_T is the measure of product quality in terms of temperature history, r is the weight factor, x is the state of cure, n is the number of state of cure observation points, x^{set} is the desired state of cure at observation point t , T is the temperature, m is the number of temperature observation points, T^{set} is the upper temperature limit at observation point j , $f(x, T, T_m(t))$ is the process model, $T_m(t)$ is the cure steps (temperature profile of cure media), $T_{m,l}$ is the lower limit for $T_m(t)$, $T_{m,u}$ is the upper limit for $T_m(t)$, t_{ee} is the final time, and t is the curing time (mold opening time).

The equality constraint of eq. (2) represents the process model that relates the state of cure and temperature to the cure media temperature, and the inequality constraints of eq. (3) represents the operational limits of cure media temperature. In practice, the SOC observation points are placed mainly in the parts of a tire where either over cure or under cure is likely to occur, while the temperature observation points are placed onto thermally sensitive layers like belt, steel and nylon chafer, bead wrap, and ply. The weight factor r provides additional flexibility to adjust relative significance between the two measures of product quality.

Process Model

The process model f in eq. (2) consists of heat transfer mechanisms and curing reaction kineticic. First, heat transfer taking place in a tire curing process can be described by the following second-order parabolic partial differential equations²:

$$\rho C_p \frac{T}{t} = \nabla \cdot (k \nabla T) + Q \text{ in } \Omega \times (0, t) \quad (4)$$

where

$$Q = p(-\Delta H) \frac{dx}{dt} \quad (5)$$

$$I.C.: T(z, 0) = T_0(z) \text{ in } \Omega \quad (6)$$

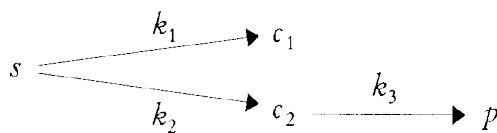
$$B.C.: T(z, t) = \hat{T}(t) \text{ on } \Omega_1 \quad (7)$$

$$-k \frac{T}{n} = h(T - T_s(t)) \text{ on } \Omega_2 \quad (8)$$

In the above equations, p denotes the density; C_p , the specific heat; k , the thermal conductivity; and h , the convective heat transfer coefficient. Q represents the rate of heat generation, which depends on the rate (do/ax) and heat (ΔH) of vulcanization of rubber compounds. Ω is the analysis domain in the spaces of z with the boundary segments Ω_1 and Ω_2 , where an essential and a natural boundary condition is prescribed, respectively.

The heat equations in eqs. (4)–(8) have several characteristics associated with tire curing processes. First, since the cure reactions of rubber compounds take place not only during the heating stage in a press but also during the cooling stage out of the press, one must solve the equations in two separate stages with the change of domain Ω in between. Next, the equations are nonlinear due to the dependence of the rubber compound properties on temperature and the state of cure. Finally, since the conditions of the cure media supplied to a bladder side or a mold side are changing according to predefined cure steps, it is necessary to model such conditions in terms of time-varying boundary conditions, as shown in eqs. (7) and (8). The other component comprising the process model f is the kinetic model for the cure reaction, which is a process of chemically producing network junctures by the insertion of crosslinks between polymer chains. The state of cure denotes the extent of the reaction and is determined by measuring the rubber properties dependent on the crosslink density. The most popular and practical method of measuring SOC is based on rheometry whereby the time-varying torque required for maintaining a given dynamic strain on a vulcanizing rubber specimen is recorded.

In this study, a cure kinetic model proposed earlier by Han et al.³ is used to explain the reversion and the induction period that are commonly found in the vulcanization of rubber compounds. The model postulates a reaction mechanism with the following three reaction paths:



where s denotes the current amount of sulfur; c_1 , the strong and stable crosslinks; and c_2 , the weak and unstable crosslinks. Once destroyed, the weak crosslinks cannot participate in the vulcanization again, thus being responsible for cure reversion.

After defining the amount of each species against the initial amount of sulfur s_0 ,

$$s^* = \frac{s}{s_0}, \quad x_1 = \frac{c_1}{s_0}, \quad x_2 = \frac{c_2}{s_0} \quad (9)$$

one can easily obtain the following rate equations:

$$\left. \begin{array}{l} | \tilde{s} = 0, x_1 = x_2 = 0 \text{ for } t < t_i \\ \left. \begin{array}{l} \frac{d\tilde{s}}{dt} = -(k_1 + k_2)\tilde{s} \\ \frac{dx_1}{dt} = k_1\tilde{s} \\ \frac{dx_2}{dt} = k_2\tilde{s} - k_3x_2 \end{array} \right\} \text{ for } t \geq t_i \end{array} \right\} \quad (10)$$

where t_i denotes the induction period. Now the sum $x = x_1 + x_2$ represents the state of cure corresponding to both the strong and weak cross-links. The temperature dependence of kinetic parameters are described by the following Arrhenius-type equations:

$$k_i = k_{i0} \exp[-E_i/RT(t)], \quad i = 1, 2, 3 \quad (11)$$

$$t_i = t_{i0} \exp[E_i/RT(t)] \quad (12)$$

B-Spline Representation of Cure Steps

The optimization problem stated in eqs. (1)–(3) is an optimal control problem in nature where the control function $T_m(t)$ that minimizes the given objective functional J is to be found. The solution of an optimal control problem is usually constructed on the basis of the Pontryagin's minimum principle⁴ derived from variational calculus. But it is simply impractical to apply the minimum principle to the distributed parameter system like ours because the partial differential heat transfer equation will result in too many state equations to handle even after rough, approximate discretization. An alternative method will be to represent the control function *a priori* as a linear combination of appropriate basis functions. This control vector parameterization renders the optimization problem finite-dimensional, where a vector of coefficients that minimize the objective function is to be found and thus allows the use of well-established multivariate optimization techniques, no matter how complex the process model may be.

In this study, the control vector $T_m(t)$ is parameterized using B-splines as follows. First, a given curing time interval $[t_{\min}, t_{\max}]$ over which optimal cure steps are to be found is divided into subintervals to define a break point sequence $b = (b_1, b_2, \dots, b_{l+1})$ satisfying

$$t_{\min} = b_1 < b_2 < \dots < b_l < b_{l+1} = t_{\max} \quad (13)$$

Next are chosen the order k of piecewise polynomials to be defined on each subinterval and the number of continuity conditions v to be imposed at each of the interior break points, b_2, \dots, b_l . The space $P_{k,b,v}$ of piecewise polynomials thus defined is a linear space with the dimension N

$$= (k - v)l + v, \text{ and its basis is called the}$$

B-splines.⁵ The specification l, k, v of the space

$P_{k,b,v}$ is used to generate a knot sequence ϕ

$$= [\phi_1, \dots, \phi_{N+k}] \text{ which satisfies the following: (1) } \phi_1 = \dots = \phi_k = b_1, b_{l+1} = \dots = \phi_{N+k}; \quad (2)$$

b_2, b_3, \dots, b_l are placed $(k - v)$ times, respectively.

Then, the i th spline $B_i(t)$ is defined as follows:

$$B_i(t) = (\phi_{i+k} - \phi_i)[\phi_i, \dots, \phi_{i+k}](r - t)^{k-1} \quad (14)$$

where $[\phi_i, \dots, \phi_{i+k}]$ denotes the k th divided difference with respect to the dummy variable r and $(r - t)^{k-1}$ denotes a truncated power function of order k as follows:

B-splines.⁵ The specification l, k, v of the space $P_{k,b,v}$ is used to generate a knot sequence ϕ

$$= [\phi_1, \dots, \phi_{N+k}]^+ \text{ which satisfies the following: (1) } \phi_1 = \dots = \phi_k = b_1, b_{l+1} = \dots = \phi_{N+k}; \quad (2)$$

b_2, b_3, \dots, b_l are placed $(k - v)$ times, respectively.

Then, the i th spline $B_i(t)$ is defined as follows:

$$B_i(t) = (\phi_{i+k} - \phi_i)[\phi_i, \dots, \phi_{i+k}](r - t)^{k-1} \quad (14)$$

where $[\phi_i, \dots, \phi_{i+k}]$ denotes the k th divided difference with respect to the dummy variable r and $(r - t)^{k-1}$ denotes a truncated power function of order k as follows:

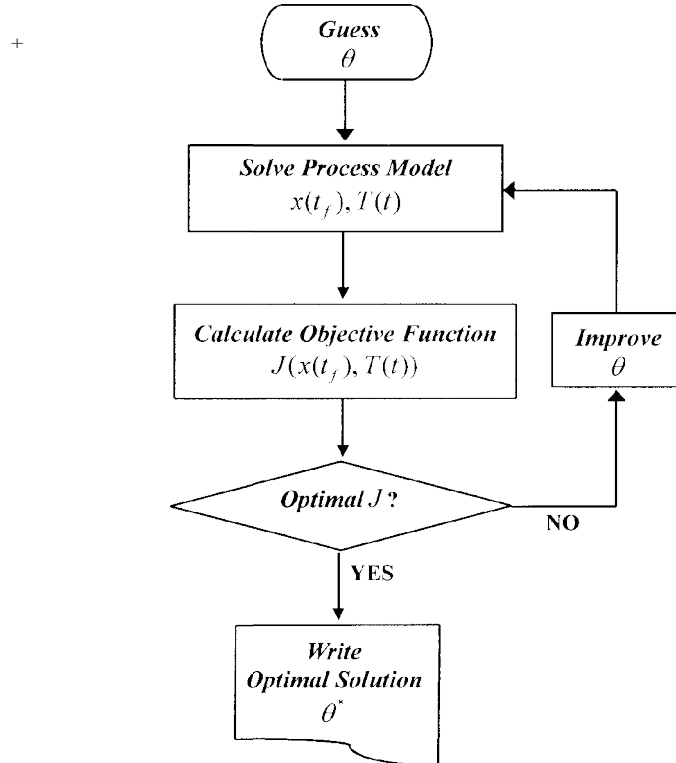


Figure 2 Numerical optimization procedure.

NUMERICAL ALGORITHMS

Our numerical algorithm for solving the optimization problem in eqs. (1)–(3) using the B-splines parameterization of eq. (16) consists of the following two major modules: (1) a solver that computes the solutions of the heat transfer equation and the cure rate model for a given vector θ of B-spline coefficients, and (2) an optimization algorithm that finds the optimal vector θ^* that minimizes the objective function J . Figure 2 depicts the iterative solution procedure and the interconnection between the two modules.

The solver for the process model was constructed on the basis of the finite element method. The numerical algorithm, code development, and execution procedure are presented in detail in our previous study,⁷ which aimed at developing a rigorous dynamic simulator for the tire curing processes. A major change introduced in the present study is the fourth-order Runge–Kutta method for solving the reversion-type cure model of eq. (10) that replaces the nonreversion type cure kinetics employed in the previous study.⁷

The constrained optimization problem with respect to θ was solved using the complex method,⁸ which extends the simplex method to problems with inequality constraints. The complex method is a direct method that only uses the function values and does not require the gradients of an objective function. Although direct methods are generally believed to be less efficient than gradient-based methods like quasi-Newton or successive quadratic programming methods, the complex method was found to outperform the latter methods for our problem. This is because the objective function J is not differentiable at some values of θ due to the induction period t_i in the cure kinetic model; thus, the gradient-based methods fail to provide reliable improvement of θ in the neighborhood of such singular points

Table I Properties of the Rubber Compounds for the TBR Tire

Compound No.	Thermal Conductivity ($J \text{ min}^{-1} \text{ cm}^{-1} \text{ } ^\circ\text{C}^{-1}$)		Density (g cm^{-3})		Specific Heat ($J \text{ g}^{-1} \text{ } ^\circ\text{C}^{-1}$)				Vulcanization ($J \text{ g}^{-1}$)
	a	$b \times 10^4$	ρ_c	ρ_u	a_c	$b_c \times 10^4$	a_u	$b_u \times 10^4$	
1	0.2046	-3.24	1.2343	1.2294	1.7943	7.48	1.1707	59.00	-1.534
2	0.1603	-2.04	1.1066	1.1026	2.0944	3.59	1.0460	102.86	-8.351
3	0.2046	-3.24	1.1624	1.1594	1.9486	4.31	0.8698	120.59	-4.480
4	0.2056	-1.08	2.4422	2.4422	1.0060	4.38	0.5971	48.45	-1.700
5	0.1603	-2.04	1.1066	1.1026	2.0944	3.59	1.0460	102.86	-8.351
6	0.1688	-1.62	1.1071	1.1035	1.1671	55.32	1.0702	97.09	-4.773
7	0.2247	-2.10	2.2423	2.2423	0.9861	8.51	0.7548	29.93	-6.531
8	0.1513	-1.98	1.1088	1.1061	2.0359	-0.27	1.1601	81.30	-10.883
9	0.2104	-4.92	1.0921	1.0921	2.4131	-12.72	1.7457	45.21	-10.880
10	0.1513	-1.98	1.1088	1.1061	2.0359	-0.27	1.1601	81.30	-10.883
11	0.1982	-0.516	1.9557	1.9557	1.0718	9.14	0.8048	33.87	-7.538
12	0.1728	-1.44	1.0910	1.0910	1.9243	0.62	0.8949	122.88	-17.168
13	1.0769	231.42	7.4767	7.4767	0.5126	4.47	0.5230	3.95	-0.209
14	0.1673	-1.86	1.1223	1.1169	2.0007	5.33	2.0672	9.88	-24.076
15	0.1872	-2.10	1.2008	1.1909	1.6902	13.70	1.1656	62.27	-14.809
16	0.1495	-1.38	1.1403	1.1065	1.8347	11.16	2.3481	-28.40	-6.458

MODEL PARAMETERS ESTIMATION

The three thermal properties (k , p , C_p) of rubber compounds appearing in eq. (4) are dependent on temperature and/or the SOC. In this article, the dependency of these properties are modeled as follows.⁷

$$k(T) = a + bT \quad (17)$$

$$p(x) = (1 - x)p_u + xp_c \quad (18)$$

$$C_p(T, x) = (1 - x)C_{pu}(T) + xC_{pc}(T) \quad (19)$$

where the subscript u indicate an uncured state ($x = 0$) and c a fully cured state ($x = 1$). The coefficients in eqs. (17), (20), and (21) were determined from linear regression of the experimental values measured at several temperatures. Table I lists the values or the regressed coefficients of the properties of 16 rubber compounds comprising the TBR tire, for which the cure optimization procedure is demonstrated below.

The frequency factors and activation energies appearing in eqs. (11) and (12) were estimated on the basis of rheometry experiments. The measured torque curves were related to the SOC profiles as follows where Γ_0 denotes the initial torque and Γ_m , the hypothetical maximum torque that would be obtained at the fully cured state. First, the least-squares method was used to find the three rate constants (k_1 , k_2 , k_3) and the induction period (t_i), along with Γ_0 and Γ_m that best fit an isothermal rheometer curve. This nonlinear regression step was repeated for several temperatures. Then from the Arrhenius plot of the estimated k_i 's and t_i 's versus temperature, the frequency factor and the activation energy of each parameter were determined. Table II lists the estimated cure kinetic parameters for the 16 rubber compounds shown in Table I.

NUMERICAL SIMULATION

The optimization algorithm was applied to the problem of determining optimal cure steps for a TBR tire in a dome type press. Figure 3 shows a quarter cross section of the axisymmetric press assembly and the structure of the layers in the TBR tire. The thermal and cure kinetic parameters of the 16 rubber compounds comprising the tire are listed in Tables I and II, respectively. Figure 4(a) shows the time-varying temperatures of the cure media supplied to the dome side and the bladder side, respectively, during a pilot test for determining the cure steps for the tire.⁷ The initial 2-min period represents a shaping period during which the green tire is pressed against the mold by high-pressure steam to ensure the correct tread pattern to be realized. The cure media are gradually drained with the temperature falling to 104°C for several minutes before the mold is open at t_h . Here, the optimal curing problem is assumed to consist of determining the optimal temperature profile of the bladder side cure media after the shaping period until the mold opening time. This situation is depicted in Figure 4(b).

The objective function formulated in eq. (1) was used in our simulation with $n = 18$ and $m = 30$. The 18 SOC observation points were assigned to the center (5 points), shoulder (5 points), sidewall (3 points), and hump (5 points) section, respectively, with x^{set} uniformly set equal to 1 (see Fig. 3). Six temperature observation points were placed evenly along each of the following heat-sensitive layers: belt (145°C), steel chafer (145°C), bead wrap/bundle (145°C), nylon chafer (193°C), and ply (152°C), where the temperatures in parentheses denote the temperature limits for respective layers. The temperature of the bladder side cure media was assumed to be adjustable between 100 and 212°C. To solve the heat transfer model shown in eqs. (4)–(8), a finite element mesh was generated for the analysis domain shown in Figure 3. The mesh

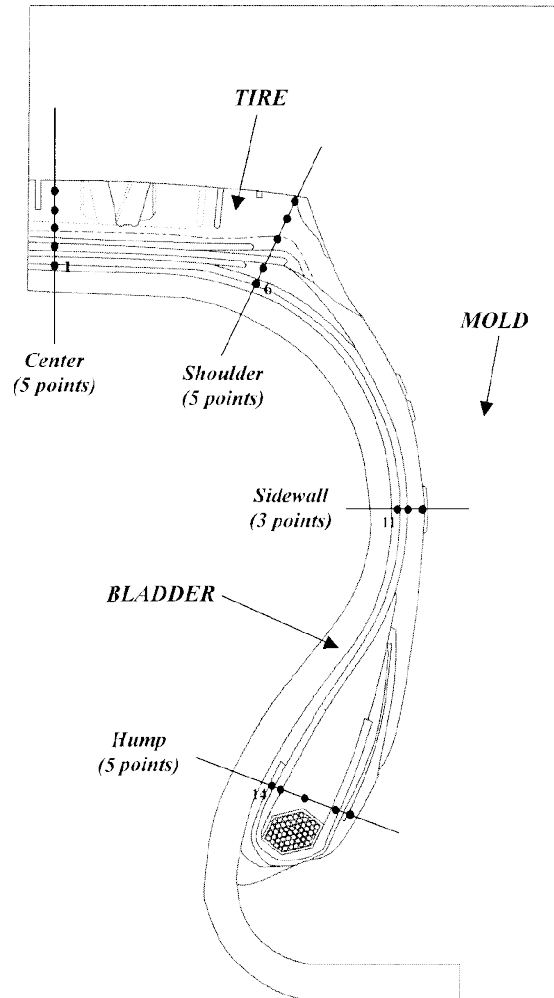


Figure 3 A quarter cross section of the cure press.

consists of 1001 axisymmetric quadrilateral elements, 36 triangular elements, 1072 nodes, and 18 materials. At the cooling stage after the mold is open, the mesh for the tire section only was retained for solving the model until $t_f = 130$ min.

The B-spline specification $l = 3$, $k = 4$, and $v = 3$

was used to represent the cure media temperature $T_m(t)$, leading to a six-element spline coefficient vector θ . It should be noticed, however, that θ_1 and θ_6 are constrained at 168 and 104°C, respectively, during optimization because of the aforementioned shaping and drain conditions.

Table III summarizes the execution status of the optimization runs carried out in this study. The first row lists the values of objective functions for the pilot cure steps shown in Figure 4(a), and the other rows list those for the cure

steps optimized with different sets of curing time and weight factor. Figure 5(a) compares the pilot cure steps with the optimal cure steps for the same curing time of 50 min and weight factor of 1, and Figure 5(b) compares the respective final states of cure at the observation points numbered from the bladder side in each section of the tire. Except for an initial 10-min period, the optimal cure steps show much lower temperature profile than the pilot steps. The optimized profile led to a higher SOC profile in each section than the pilot steps in Figure 5(b) and, accordingly, to a smaller J_x value in Table III. The difference in the SOC values between two cure steps is more salient at the observation points near the bladder than the mold side observation points because only the bladder side cure steps were optimized in this study. The lower SOC values for the pilot steps resulted from the overcure caused by the excessively high-temperature profile of bladder side cure media. This can be confirmed in Figure 6, which compares the temporal progress of SOCs at observation points 1 and 2 in the center section between the pilot and optimal cure steps. Besides the lower SOC values, the pilot steps must have caused the heat-sensitive layers to violate the respective temperature limits to a considerable degree, as manifested by the much larger value of J_T in Table III.

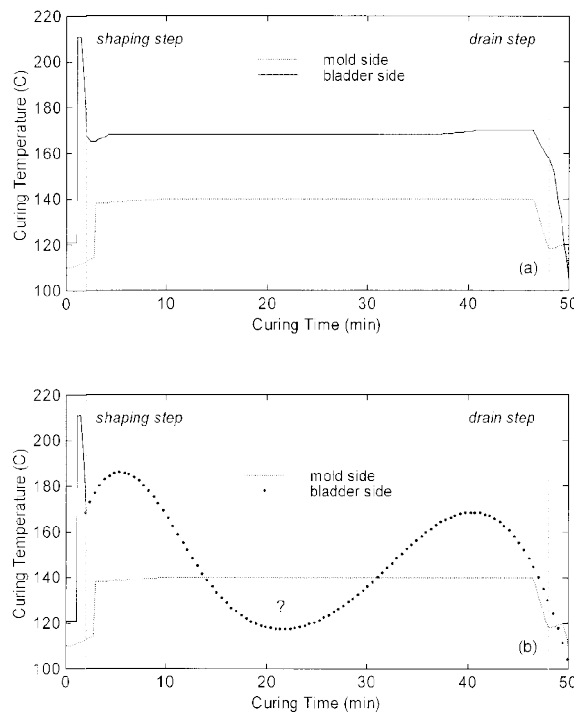


Figure 4 Temperature profiles of the cure media during cure of a TBR tire: (a) pilot test; (b) to be optimized.

Table III Execution Status of the Cure Optimization Runs

Run No.	t_c (min)	r ($^{\circ}\text{C}^{-2} \text{min}^{-1}$)	J_x (-)	J_T ($^{\circ}\text{C}^2 \text{min}$)	J (-)	No. of Function Evaluations
Pilot	50	1	1.8572×10^{-2}	9.6296×10^1	9.6315×10^1	—
1	50	1	1.1781×10^{-2}	2.0638×10^{-7}	1.1781×10^{-2}	316
2	50	0	1.1521×10^{-2}	3.4915	1.1521×10^{-2}	250
3	50	10	1.1858×10^{-2}	6.3755×10^{-9}	1.1858×10^{-2}	367
4	40	1	2.0454×10^{-2}	5.0948×10^{-6}	2.0459×10^{-2}	464
5	60	1	1.0670×10^{-2}	1.0276×10^{-6}	1.0671×10^{-2}	363

Figure 7 shows the effect of the weight factor on the optimal cure steps (runs 1, 2, and 3). Run 2 corresponds to the case where the penalty to excessive temperature was ignored in the actual optimization procedure. As a result, the smallest J_x was obtained among the three runs but with a many orders-of-magnitude larger value of J_T . When the temperature penalty term was actually introduced, the curing temperature showed milder excursions, but the final SOC profiles did not exhibit significant differences.

Figure 8 shows the effect of the curing time on the optimal cure steps (runs 1, 4, and 5). When

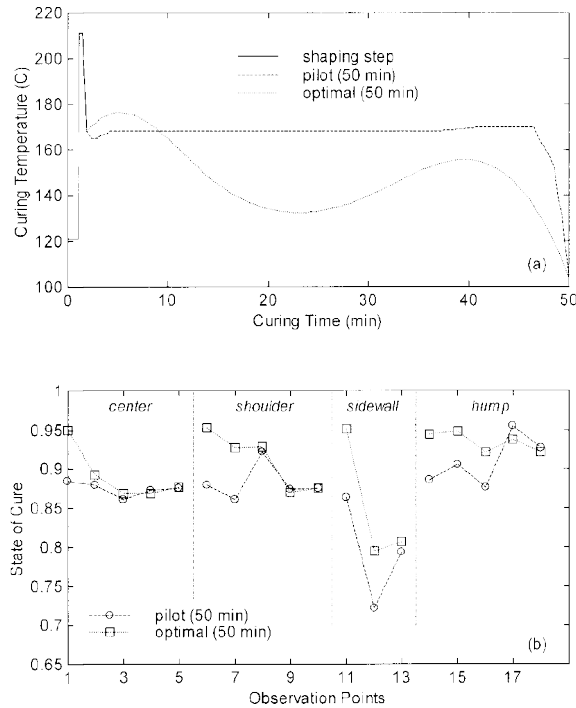


Figure 5 Comparison of pilot versus optimal cure steps: (a) temperature profiles of the bladder side cure media; (b) final states of cure at the SOC observation points

the mold was opened 10 minutes earlier than the nominal case, the optimal temperature showed sharp increase as expected in order to prevent the undercure of rubber compounds. Although this elevated temperature of bladder side cure media helped the adjacent layers to reach SOC levels comparable to those obtained at longer cure time, the innermost or mold side layers suffered from undercure due to insufficient curing time. When the mold opening time was prolonged to 60 min, the optimal cure steps showed initial decrease until about 15 min, followed by a gradual peak. The lower curing temperature for longer time was necessary to prevent the overcure and, in fact, was more favorable to higher states of cure, as manifested by smaller J_x values in Table III and higher SOC profiles in Figure 8(b). It should be noted, however, that longer cure time means decreased productivity; hence, trade-offs should be made between product quality and productivity.

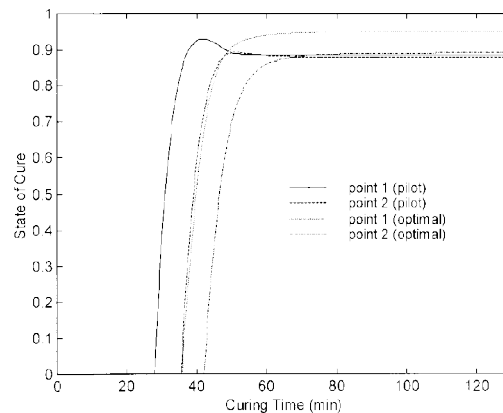
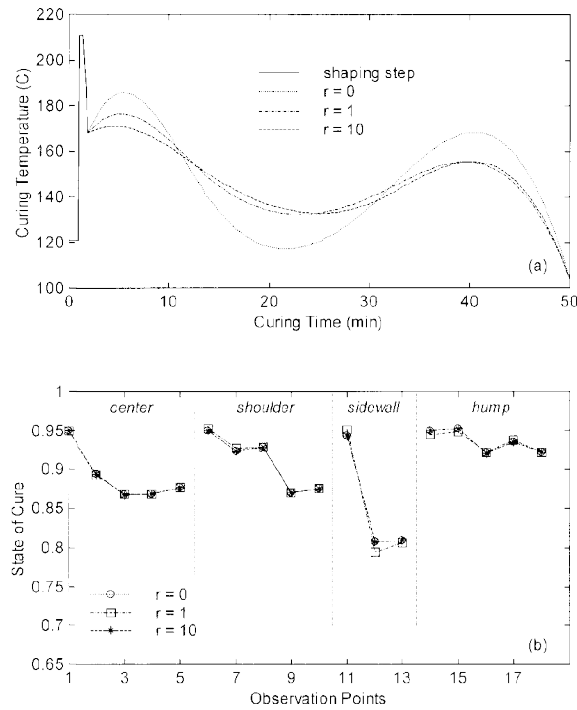


Figure 6 Temporal progress of SOC at observation points 1 and 2 for the pilot and optimal cure steps (run 1).



II. CONCLUSION

A systematic procedure was presented to determine optimal cure steps for product quality in a tire curing process. First, the product quality was formulated into an objective function that measures the deviation of final states of cure from the target values and the violation of temperature limits prescribed for heat-sensitive composite layers. Then, the objective function was minimized under an equality constraint representing the process model and under inequality constraints representing the operational temperature limits of cure media. Next, the time-varying profile of cure media temperature was discretized using B-splines. The re-sulting dynamic optimization problem was solved using a complex algorithm along with a finite element model solver. Finally, numerical simulation results were presented to demonstrate the procedure of determining the optimal cure steps for a TBR tire.

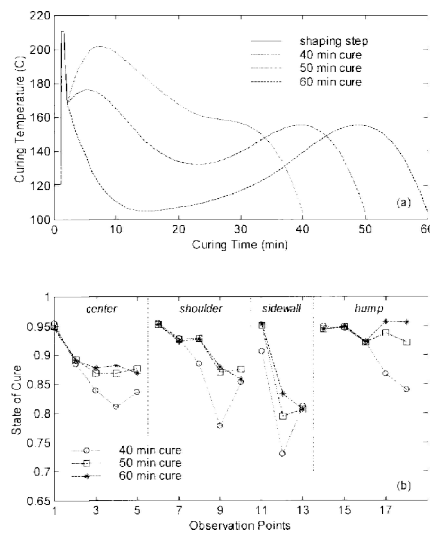


Figure 7 Effect of weight factor in optimal curing of the TBR tire: (a) temperature profiles of the bladder side cure media; (b) final states of cure at the SOC observation points.

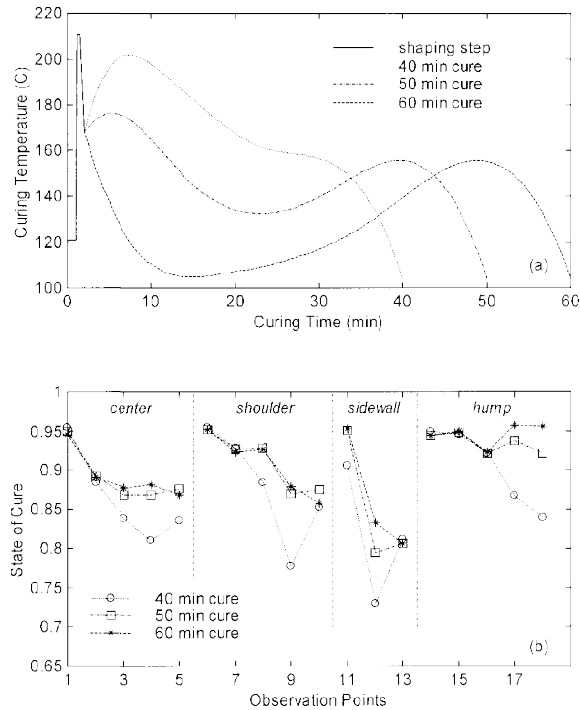


Figure 8 Effect of curing time in optimal curing of the TBR tire: (a) temperature profiles of the bladder side cure media; (b) final states of cure at the SOC observation points.

This study was supported by Kumho Tire Co., Ltd., Korea, and the authors thank the company for permission to publish the study.

REFERENCES

- [1]. Toth, W. J.; Chang, J. P.; Zanichelli, C. *Tire Sci Technol* 2020
- [2]. Holman, J. P. *Heat transfer*, 5th ed.; McGraw-Hill: New York, 2021
- [3]. Han, I.-S.; Chung, C.-B.; Lee, J.-W. *Rubber Chem Technol* to appear.
- [4]. Pontryagin, L. S.; Gamkrelidze, V. G.; Mishenko, E. F. *The Mathematical Theory of Optimal Processes*; Brown, D. E., trans.; Macmillan: New York, 2016.
- [6]. de Boor, C. *A Practical Guide to Splines*; Springer-Verlag: New York, 2022
- [7]. Becker, E. B.; Carey, G. F.; Oden, J. T. *Finite Elements, Vol. I*; Prentice Hall: New York, 2015.
- [8]. Han, I.-S.; Chung, C.-B.; Kim, J.-H.; Kim, S.-J.; Chung, H.-C.; Cho, C.-T.; Oh, S.-C. *Tire Sci and Technol* 2013
- [9]. Rao, S. S. *Engineering Optimization: Theory and Practice*; John Wiley & Sons: New York, 2019

BIOGRAPHICAL NOTES



Mr. N.J. VADERA is P.G. Research Scholar at Government engineering college, DAHOD and pursuing M.E. CAD/CAM 1st Year. He has completed his B.E. from GEC, GODHRA in 2019. His area of research is automation, production systems, CAM.



Dr.D.B. JANI received PH.D. In Thermal Science (Mechanical Engineering) from Indian Institute of Technology (IIT) ROORKEE. Currently, he is recognized Ph.D. supervisor at Gujarat Technological University (GTU), Ahmadabad. He has published more than 180 Research Articles in International Conferences and Journals including reputed books and book chapters. Presently, he is an Associate Professor at GEC, DAHOD Gujarat Technological University, GTU, Ahmadabad (Education Department, State of Gujarat, India, Class-I, Gazetted Officer). His area of research is Desiccant cooling, ANN, TRNSYS, Energy.



DR.S.B.DIKSHIT Currently Working as Assistant Professor in the Department Of Mechanical Engineering at Government Engineering College DAHOD under the Gujarat Technological University. His Area Of Interest Is Thermal Engineering, IC Engine And Automobile And Manufacturing